

Appendix

Model Calibration

Calibration of TEM-Hydro involves adjusting several parameters to get the site specific (targeted) carbon in vegetation and soils such as total vegetation and soil carbon, GPP, Nitrogen-limited Net Primary Production (NPP), nitrogen-saturated NPP, and available inorganic nitrogen. The model is calibrated to develop parameter values for photosynthesis (c_{max}), uptake of inorganic nitrogen (n_{max}), maintenance respiration (k_r), heterotrophic respiration (k_d), and vegetation carbon ($\tau_{heartwood}$). Our calibration sites are Harvard Forest, MA for temperate deciduous forest (oak, maple) and temperate coniferous forest (pine), Bonanza Creek, AK for boreal forest (spruce), Pawnee grasslands, CO, a predominantly C4 short grassland, and Curlew shrubland, UT, a mixed C3 deciduous and C4 evergreen shrubland. For C3 vegetation we assume a half saturation constant (k_c) of 200 for the effects of CO_2 fertilization, consistent with [Felzer *et al.*, 2009]. For C4 vegetation we assume a low k_c value of 40. We assume Pawnee is a 30/70 C3/C4 mix and Curlew is 50/50. Final calibrated values are given in the **Table A1**. Other biome-dependent parameters are given in **Table A2** and biome independent parameters in **Table A3**. Target carbon and nitrogen stock and flux values for each biome are given in **Table A4**. USGS stream gauges used for validation are given in **Table A5**.

Running Means: Many new variables are running means; the timescale used to calculate them is based on the characteristic timescale for turnover of living plant tissue. Some of the specific usages of running means are included in the descriptions below.

Canopy Conductance: The canopy conductance (g_c) is according to Ball *et al.* [1987]:

$$g_c = g_{s_{min}} \times LAI + g_{s_a} \frac{GPP \times RH}{C_a}$$

$$g_s = \frac{g_c}{LAI}$$

where $g_{s_{min}}$ is minimum stomatal aperture ($mmol\ m^{-2}\ s^{-1}$), g_{s_a} is the stomatal slope (unitless), LAI is the leaf area index, GPP is the Gross Primary Productivity, RH is the relative humidity, C_a is the ambient carbon dioxide concentration, and g_s is the average stomatal conductance.

Aerodynamics and Windspeed: To better account for the effects of broad climatological variations in windspeed on surface energy fluxes, we now read in a windspeed dataset. This is used, together with vegetation height, to determine aerodynamic resistances within the soil-canopy-atmosphere system. These aerodynamic resistances are used in the Shuttleworth and Wallace [1985] evapotranspiration formula. The formulations below are from Choudhury and Monteith [1988], Federer *et al.* [1996] and Zhou *et al.* [2006].

$$rac = \frac{100.0 \times neddy \times (wleaf \times k_karman)^{0.5}}{2.0 \times LAI \times (u^* \times \log(zh - zd)/zo)^{0.5} \times (1.0 - \exp(-0.5 \times neddy))} \quad (1)$$

$$ras = \frac{zh \times \exp(neddy) \times (1.0 - \exp(-neddy \times [zd + zo]/zh))}{k_karman \times u^* \times neddy \times (zh - zd)} \quad (2)$$

$$raa = \frac{zh \times (\exp[neddy \times (1.0 - (zd + zo)/zh) - 1.0]/[neddy \times (zh - zd)]) + \log([za - zd]/[zh - zd])}{u^* \times k_karman} \quad (3)$$

where rac = leaf-to-canopy aerodynamic resistance, ras = soil-to-canopy aerodynamic resistance, raa = canopy-to-screen height aerodynamic resistance, $wleaf$ = biome-dependant parameter, and

$$ua = u \times \frac{\log(296.97/0.005)}{\log(296.97/zo)} \times \frac{\log([za - zd]/zo)}{\log(10.0/0.005)}$$

$$zh = href \times cabove^{kallom}$$

$$za = zh + 2.0$$

$$zd = \min\left(1.1 \times zh \times \log\left[1.0 + (0.1 \times LAI)^{0.25}\right], 0.9 \times zh\right)$$

$$zo = 0.3 \times zh \times \min\left(0.01 + (0.1 \times LAI)^{0.5}, 1 - zd/zh\right)$$

$$u^* = k_karman \times ua / \log([za - zd]/zo)$$

$$neddy = 2.306 + 0.194 \times zh$$

where ua = windspeed at 2 m above the canopy, zh = canopy height, za = reference height 2 m above canopy, zd = displacement height, u^* = friction velocity, and $neddy$ = eddy resistance coefficient. The friction velocity depends on the windspeed and roughness length (zo). The roughness length depends on the canopy density and canopy height. The displacement height depends on the canopy height and LAI. Other variables are: u = windspeed at 10 m height, $href$ = biome-dependent reference height, $kallom$ = biome-dependent parameter, $cabove$ = total above ground biomass in $kg\ C\ m^{-2}$, $k_karman\ constant = 0.41$. The canopy aerodynamic resistance (rac) decreases as LAI and u^* increase; the more air is moving through a denser canopy, the more coupled the canopy is to the air. N_{eddy} is related to a turbulent closure parameterization; as

81 it increases with vegetation height, the soil is more and more cut off from the atmosphere (e.g. r_{as}
 82 becomes larger).

83
 84

85 **Internal Leaf CO₂:** The internal leaf CO₂ (c_i) is now consistent with the calculation of GPP and
 86 stomatal conductance, assuming that the CO₂ on the leaf surface is equal to the atmospheric
 87 CO₂. The equations to be solved for c_i simultaneously are:

$$88 \quad GPP = cmax \times fpar \times temp \times fozone \times fh2o \times \frac{c_i}{k_c + c_i} = fp \times \frac{c_i}{k_c + c_i} \quad (4)$$

89

$$90 \quad GPP = \frac{gc}{1.563} (c_a - c_i) \quad (5)$$

91

$$92 \quad gc = gsmin \times LAI + \frac{gsa \times (GPP - r_l) \times RH}{c_a} \quad (6)$$

93

94 where $cmax$ = maximum leaf-level photosynthetic rate, $fpar$ = canopy integrated light response
 95 function, $temp$ = GPP dependence on temperature, kc = half-saturation constant of CO₂
 96 fertilization, 1.563 = ratio of molecular diffusivity of water vapor to carbon dioxide ((44/18)^{0.5}),
 97 c_a = atmospheric CO₂ level, $gsmin$ = minimum stomatal aperture (mmol m⁻² s⁻¹), gsa = stomatal
 98 slope, r_l = leaf growth and maintenance respiration (mmol m⁻² s⁻¹), and RH = relative humidity.
 99 The simultaneous solution of c_i involves the solution to a quadratic equation. The solution is:

100

$$101 \quad a = -gsmin \times LAI * c_a \times (GPP - r_a)$$

102

$$103 \quad b = c_a \times (gsa \times fd - 1.563) \times (GPP - r_a) + gsa \times RH \times r_a \times k_c + gsmin \times LAI \times c_a \times (c_a - k_c)$$

104

$$c = c_a \times k_c \times (gsmin \times LAI * c_a - r_a \times (gsa \times RH - 1.563))$$

106

$$107 \quad c_i = \frac{-b - \left([b^2 - 4 \times a \times c]^{0.5} \right)}{2 \times a}$$

108

109 This solution can be thought of graphically by plotting the equation for GPP from (4) together
 110 with the equation for GPP from (5) and (6) (after eliminating gc), as the dependent variable, with
 111 the independent variable being c_i . c_i tends to lie in between c_a and 0; though for $r_a > GPP$, it
 112 may be larger. When the $gsmin \times LAI$ term and r_l are negligible in equation (6), this expression
 113 tends toward the open-stomata limit used in Felzer et al. [2009].

114

115

116

117 **Canopy Interception:** Canopy interception is now explicitly calculated, along with soil
 118 evaporation and transpiration. Canopy interception is a function of precipitation and LAI.

119
 120 $can_{int} = ndays \times (1.0 - \exp(-0.005 \times prec)) * (1.0 - \exp(kext \times LAI)) \times 0.1 \times LAI$ (7)

121
 122 where $ndays$ = number of days in a month, $prec$ = precipitation, and $kext$ = biome-dependent
 123 extinction coefficient. The energy flux associated with this term is subtracted from the net
 124 radiation in the evapotranspiration computation. This term can be thought of as something like a
 125 product of the number of rain events $n_{rain} \sim \{ndays \times (1 - \exp(-0.005 \times prec))\}$, the probability of a
 126 raindrop hitting a leaf $p_{int} \sim \{1.0 - \exp(kext \times LAI)\}$, and the total evaporative capacity of the
 127 canopy per rainfall event $e_{int} \sim (0.1 \times LAI)$. Thus, a wet region with 100 mm month⁻¹ of rain
 128 ($n_{rain} \sim 12$) and an LAI of 4 ($p_{int} \sim 0.9$, $e_{int} \sim 0.4$) would intercept ~ 4 mm month⁻¹. A more
 129 thorough treatment (many exist) would consider the evaporative demand of the atmosphere and
 130 would track the stock of leaf-surface water explicitly, but we lack the temporal resolution (in
 131 data and other model equations) to perform such calculations. Parameters in the equation,
 132 especially the “0.1”, could be modified to attempt to better fit data.

133
 134
 135 **Day-Night disaggregation:** Energy fluxes and photosynthesis are computed separately for day
 136 and night. This requires use of a diurnal temperature range dataset, and calculation of day and
 137 night temperature, vapor pressure deficit, and longwave radiation.

138
 139 Photosynthesis Detailed description is in Felzer et al. [2009]. The temperature term, f_T , now
 140 uses the daytime temperature. The canopy conductance, based on Ball et al. [1987] and the
 141 related internal CO₂, is now a function of relative humidity rather than a hyperbolic function of
 142 vapor pressure deficit, so that is now calculated from using daytime temperature. The
 143 photosynthetically active radiation (PAR) is an average daytime value.

144
 145 Canopy Conductance As detailed above, the moisture dependency is based on relative humidity,
 146 which is calculated from vapor pressure and daytime and nighttime temperature.

147
 148 Evapotranspiration Evapotranspiration is calculated using the Shuttleworth and Wallace [1985]
 149 approach. Terms that now include day and night differentiation include net radiation, including
 150 soil and snow storage, the rate of change of vapor pressure with temperature (β), which depends
 151 upon both temperature and vapor pressure deficit, and vapor pressure deficit itself. Daytime and
 152 nighttime temperature and vapor pressure deficit (calculated from the vapor pressures and
 153 respective temperatures) are used. In addition, emitted longwave radiation is subtracted from the
 154 net radiation term (rn) and from the soil radiation (rn_{soil}), and that is based upon daytime and
 155 nighttime temperature according to the Stefan-Boltzmann Law.

156
 157 $lw = \left(1.0 - 1.24 \times \frac{vpr^{1.0/7.0}}{T} \right) \times cor \times \sigma \times T^4 + ecan + esoil$

158 $cor = 1.6 \times \frac{nirr}{girr} - 0.2$

159 where vpr = vapor pressure, T = temperature in K, σ = Stefan-Boltzman constant, $ecan$ =
 160 evaporation from canopy interception in W/m², $esoil$ = soil evaporation in W/m², and $cor = 0.2$

161 or 1.0 depending upon how surface radiation compares to top-of-atmosphere radiation
 162 [Brutsaert, 1982; Federer et al., 1996].

$$163$$

$$164 \quad r_{soil} = 0.8 \times ([1 - \alpha] \times nirr - lw) \times \exp(-k_{ext} \times LAI) \quad (8)$$

$$165$$

$$166 \quad rn = nirr \times (1.0 - \alpha) - lw \quad (9)$$

167
 168 where α = biome-dependent albedo, which is 0.5 for snowcover and $nirr$ = incoming shortwave
 169 radiation at the surface.

170
 171
 172 **Soil Evaporation Limitation:** A limitation is applied to soil evaporation if available water is
 173 much smaller than the field capacity and the soil evaporation is much larger than the
 174 precipitation.

175
 176 If[(availh2o < 0.5 x awcap) and (evap > 0.5 x prec)] then

$$177$$

$$178 \quad esoil = 0.5 \times prec \quad (10)$$

179
 180 where $evap$ = soil evaporation calculated from SW approach and $esoil$ = evaporated soil water in
 181 mm. This equation is derived heuristically and is included to ensure that available water does
 182 not become negative.

183
 184
 185 **Drought-stress Function:** Roots and stems are required for water transport, and thus more
 186 allocation to them should carry benefits for reducing drought stress. These marginal benefits are
 187 calculated based on a new drought-stress formula and the marginal benefits vs costs of roots and
 188 stems are used to drive allocation.

$$189$$

$$190 \quad fh2o = 1.0 - \exp(-[lsc/lsc\ min] \times wfrac) \quad (11)$$

$$191$$

$$192 \quad lsc = \frac{gstem \times stemc \times groot \times rootc}{(gstem \times stemc + groot \times rootc) \times LAI}$$

$$193$$

$$194 \quad gstem = \frac{kstem}{1000 \times rhostem \times zh^2}$$

$$195$$

$$196 \quad wfrac = \frac{availh2o}{awcap}$$

$$197$$

198 where lsc = leaf specific conductance ($\text{mmol m}^{-2} \text{s}^{-1} \text{MPa}^{-1}$), $lscmin$ = biome-dependent
 199 minimum lsc , $gstem$ = above-ground hydraulic conductance ($\text{mmol m}^{-2} \text{s}^{-1} \text{MPa}^{-1}$), $kstem$ =
 200 biome-dependent sapwood hydraulic conductivity ($\text{mmol m}^{-1} \text{s}^{-1} \text{MPa}^{-1}$), $rhostem$ = biome-
 201 dependent stem density (g m^{-3}), $groot$ = biome-dependant root hydraulic conductance (mmol gC^{-1})

202 $^1 \text{ s}^{-1} \text{ MPa}^{-1}$), *stemc* = total stem carbon, *rootc* = total root carbon, *availh2o* = total soil moisture,
 203 *awcap* = water capacity, which is difference between field capacity and wilting point, now
 204 calculated from the Saxton equations [Saxton *et al.*, 1986] based on soil texture, and discussed
 205 below. These terms are used in the calculation of GPP and internal CO_2 (*fh2o*), and the marginal
 206 benefits of leaves (*fh2o*), stems, and roots (*lsc*, *wfrac*). For grasslands we developed an alternate
 207 function:

$$209 \quad wfrac' = wfrac \times \left(\frac{wfrac}{(0.01 + wfrac)} \right)^2$$

$$210 \quad fh2o' = 1.0 - \exp\left(-[lsc/lsc \text{ min}] \times wfrac^2\right)$$

211
 212 In this case, *wfrac'* has both zero value and zero derivative as *wfrac* goes to zero. This
 213 function GPP to approach zero more smoothly as *wfrac* approaches zero.
 214
 215

216
 217 **Saxton Equations:** Soil texture of wilting point and field capacity based on Saxton equations
 218 [Saxton *et al.*, 1986].
 219

$$220 \quad pota = 100.0 \times \exp(-4.396 - 0.0715 \times pclay - 0.000488 \times psand^2 - 0.00004285 \times psand^2 \times pclay)$$

$$221 \quad potb = -3.14 - 0.00222 \times pclay^2 - 0.00003484 \times psand^2 \times pclay$$

$$222 \quad fldcap = rootz \times 1000.0 \times \left(33.0/pota\right)^{\frac{1.0}{potb}} \quad (12)$$

$$223 \quad wiltpt = rootz \times 1000.0 \times \left(1500.0/pota\right)^{1/potb} \quad (13)$$

224
 225
 226 **Optimal Temperature for Photosynthesis:** The optimum temperature for photosynthesis (*topt*)
 227 in stress-deciduous biomes (i.e. grasslands) is now based on the running mean temperature
 228 during the growing season rather than the maximum temperature during the year to allow for
 229 lower optimum temperatures in cold grasslands, resulting in larger and more realistic
 230 productivity. The functional form is now more symmetrical about an optimum temperature for
 231 all biomes.
 232
 233

$$234 \quad pow = \frac{(topt - t \text{ min})}{t \text{ max} - topt}$$

$$235 \quad temp = \frac{\left((t \text{ max} - tair) \times (tair - t \text{ min})^{pow}\right)}{\left((t \text{ max} - topt) \times (topt - t \text{ min})^{pow}\right)} \quad (14)$$

237

238 where t_{max} and t_{min} are biome-dependent parameters. This equation has a parabolic structure,
 239 with a broad maximum, if $topt = (t_{max}+t_{min})/2$. $Topt$ is allowed to acclimate to a given climate,
 240 but as it approaches t_{max} or t_{min} , the peak of the temperature function becomes sharper. This is
 241 intended to reflect the broad temperature tolerance of a given biome, but increased specialization
 242 and sensitivity near the temperature limits of a biome. Typically, $topt > (t_{max}+t_{min})/2$, implying
 243 that $pow > 1$, and the function is concave up at low temperatures.

244
 245 **Heterotrophic Respiration Moisture Term:** In the previous version of TEM, the moisture
 246 function for heterotrophic respiration ($rhxh_2o$) depended upon volumetric soil moisture (vsm)
 247 and biome-dependent values for the minimum, maximum and optimum to define the shape of the
 248 curve. This function is based on the concept that maximum decomposition rates occur when
 249 soils are 50-80% saturated with water [Alexander, 1977; Clark, 1967], however it does not take
 250 into account differences in soil texture. Clay soils, for example, can hold more water than sandy
 251 soils, and so their larger soil moisture will result in higher respiration rates.

$$252 \quad \% \text{ porosity} = 100 \times (0.332 - 0.0007251 \times \% \text{ sand} + 0.1276 \times \log(\% \text{ clay}))$$

$$253 \quad wfps = \frac{100 \times vsm}{\% \text{ porosity}}$$

$$254 \quad rhxh_2o = \frac{0.2 + 0.8 \times wfps \times (1 - wfps)}{wfps \times (1 - wfps) + (0.6 - wfps) \times (0.6 - wfps)}$$

255
 256 where $wfps$ is the water-filled pore porosity.

257
 258
 259
 260
 261 **Nitrogen-Limitation:** In the determination of N-limiting conditions, we now use running means
 262 of labile carbon and nitrogen (to determine supply) and allocation and resorption terms (to
 263 determine demand). N-limitation occurs when both the running mean of the labile C:N is larger
 264 than the running mean of the demand C:N and the instantaneous labile C:N is larger than a target
 265 C:N. The target C:N is based on the ratio of the sum of the carbon allocations and growth
 266 respiration and labile maintenance respiration with the nitrogen labile allocations, as described in
 267 Felzer et al. [2009]. This approach allows for luxury carbon and nitrogen uptake as long as the
 268 long term C:N supply is consistent with the C:N demand and avoid combining stocks and fluxes.

$$269 \quad SupplyC : N = \frac{rlabileC}{rlabileN}$$

$$270 \quad DemandC : N = \frac{r(\sum calloc + r_g)}{r(\sum nalloc - nresorb)}$$

$$271 \quad cntar = \frac{\sum calloc + r_g}{\sum nalloc}$$

272
 273
 274
 275

276 where r indicates running means, $calloc$ = total carbon allocation to leaves, active stems, and
 277 roots, $nalloc$ = total nitrogen allocation to leaves, active stems, and roots, $nresorb$ = nitrogen
 278 resorption to leaves, and r_g = growth respiration.

279
 280 if ($SupplyC:N > DemandC:N$ and $labileC/labileN > cnprod$) then
 281

$$282 \quad GPP = \frac{DemandC : N}{SupplyC : N} \quad (15)$$

283
 284 if($SupplyN:C > DemandN:C$ and $labileN/labileC > 1/cnprod$) then
 285

$$286 \quad Nuptake = \frac{DemandN : C}{SupplyN : C} \quad (16)$$

287
 288 where $DemandN:C = 1/DemandC:N$ and $SupplyN:C = 1/SupplyC:N$.
 289

290 Nitrogen availability depends upon the incoming flux, net nitrogen mineralization, and the
 291 outgoing flux, plant nitrogen uptake. Net nitrogen mineralization is the difference between gross
 292 nitrogen mineralization and immobilization and is unchanged from earlier version of TEM
 293 [Raich *et al.*, 1991]. Gross nitrogen mineralization is the product of the ratio of soil organic
 294 nitrogen to soil organic carbon with the heterotrophic respiration. Immobilization depends upon
 295 available nitrogen and soil moisture. Nitrogen uptake depends upon temperature and is describe
 296 fully in Appendix 3 of Felzer *et al.* [2009].
 297
 298

299 **Dynamic Equilibration:** Rather than equilibrating to a long-term average climate and then being
 300 “spun up” by 3 40-year transient climate repetitions, it is now possible to equilibrate to the
 301 variability found in the observed climate timeseries. This allows interannual variability to be
 302 captured in calibration, and hopefully reduces any artifacts of the transition from spin-up to
 303 transient climate. Determination of when the model is equilibrated is now based on 40 year
 304 means of stocks rather than annual flux values, since annual fluxes generally do not equilibrate in
 305 a climate with interannual variability.
 306

307 **Carbon Benefits:** Since the expected gains in the carbon formula for GPP don’t always
 308 translate to actual gains because of N-limitation, we reduce the expected gains to account for this
 309 discrepancy. Carbon marginal benefits for all plant compartments are pro-rated by the expected
 310 ratio of running means of actual gpp to potential (non-n-limited) gpp. Also, the benefits of roots
 311 for nitrogen uptake are now accounted for, and these benefits are converted to carbon currency
 312 by the expected c:n of newly produced tissue. Nitrogen-uptake benefits of roots are pro-rated by
 313 the difference between potential gpp and actual gpp, as a fraction of potential gpp. More
 314 nitrogen limitation means a larger difference, and thus a purer benefit to increasing carbon
 315 acquisition by n uptake. If actual gpp is close to potential gpp, then the benefits to carbon
 316 acquisition of increasing n uptake are relatively small.
 317

318 **Daily Timestep and new adaptive integrator:** The model now uses a base daily timestep
 319 (though identical meteorological driving conditions are used within a month) to solve the

320 differential equations of the ecosystem. The integrator used to numerically solve has been
321 changed to the Bogacki-Shampine 2-3 order Runge-Kutta method, which requires on average 3
322 calls to delta per timestep. Run speeds are decreased, but by a factor of perhaps 2.5, not 30 as
323 might be expected. This change was implemented to allow a transition to daily data (or coupling
324 with daily output from a climate model), and to ensure numerical stability of some outputs. The
325 previous integrator contained backwards timesteps which would occasionally produce
326 unintended behavior in some of the new routines.

327
328

329 **Figures**

330

331 **Figure A1:** Moisture stress functions ($fh2o, fh2o'$) for different values of $wfrac$ and $lsc/lscmin=1$
332 and $lsc/lscmin=4$.

333

334 **Figure A2:** Moisture function for heterotrophic respiration for several different soil porosities.

335

336 **Figure A3:** TEM-Hydro carbon cycle is further divided between four vegetation structural pools
337 (fine roots, leaves, sapwood, and heartwood), and a labile pool for storage.

338

339 **Figure A4:** TEM-Hydro nitrogen cycle is further divided between four vegetation structural
340 pools (fine roots, leaves, sapwood, and heartwood), and a labile pool for storage.

341

342 **Figure A5:** Soil evaporation and plant transpiration are determined using a simple bucket model
343 with the [Shuttleworth and Wallace, 1985] approach to calculating ET.

344

345

346

347 **References**

348

349 Alexander, M. (1977), *Introduction to soil microbiology, Second Edition*, John Wiley and
350 Sons, New York, New York.

351 Ball, J. T., I. E. Woodrow, and J. A. Berry (1987), A model predicting stomatal
352 conductance and its contribution to the control of photosynthesis under different
353 environmental conditions, *Progress in Photosynthesis Research, IV*(Journal
354 Article), ISBN9024734533.

355 Brutsaert, W. (1982), *Evaporation into the Atmosphere: Theory, History, and*
356 *Applications*, 299 pp., D. Reidel, Hingham, MA.

357 Choudhury, B. J., and J. L. Monteith (1988), A four-layer model for the heat budget of
358 homogeneous land surfaces, *Quarterly Journal of the Royal Meteorological*
359 *Society, 114*(Journal Article), 373-398.

360 Clark, F. E. (1967), Bacteria in soil, in *Soil Biology*, edited by A. Burges and F. Raw, pp.
361 15-49, Academic Press, London, England.

362 Federer, C. A., C. J. Vorosmarty, and B. Fekete (1996), Intercomparison of methods for
363 calculating potential evapotranspiration in regional global water balance models,
364 *Water Resources Research, 32*(Journal Article), 2315-2321.

365 Felzer, B. S., T. W. Cronin, J. M. Melillo, D. W. Kicklighter, and C. A. Schlosser (2009),
366 Importance of carbon-nitrogen interactions and ozone on ecosystem hydrology
367 during the 21st century, *JGR-Biogeosciences*, 114(Journal Article).

368 Raich, J. W., E. B. Rastetter, J. M. Melillo, D. W. Kicklighter, P. A. Steudler, B. J.
369 Peterson, A. L. Grace, B. Moore Iii, and C. J. Vorosmarty (1991), Potential net
370 primary productivity in South America: application of a global model, *Ecological*
371 *Applications*, 1(4), 399-429.

372 Saxton, K. E., W. J. Rawls, J. S. Romberger, and R. I. Papendick (1986), Estimating
373 generalized soil-water characteristics from texture, *Soil Sci. Soc. Am. J.*, 50, 1031-
374 1036.

375 Shuttleworth, W. J., and J. S. Wallace (1985), Evaporation from sparse crops: an energy
376 combination theory, *Quarterly Journal of the Royal Meteorological Society*, 111,
377 839-855.

378 Zhou, M. C., H. Ishidaira, H. P. Hapuarachchi, J. Magome, A. S. Kiern, and K. Takeuchi
379 (2006), Estimating potential evapotranspiration using Shuttleworth-Wallace
380 model and NOAA-AVHRR NDVI data to feed a distributed hydrological model
381 over the Mekong River basin, *Journal of Hydrology*, 327(1-2), 151-173.
382
383

Table A1: TEM-Hydro Calibration parameters

description	temp. dec.	temp. conif.	boreal forest	shrub- land	grass- land	unit
maximum leaf-level assimilation rate	19.50	11.80	10.55	17.00	26.00	$\mu\text{mol CO}_2 \text{ m}^{-2} \text{ s}^{-1}$
stem mortality	54.75	56.00	140.00	13.00	2.30	years
autotrophic respiration coefficient	0.3400	0.2200	0.5000	0.2600	0.1400	$\mu\text{mol CO}_2 \text{ gN}^{-1} \text{ s}^{-1}$ at topt
heterotrophic respiration coefficient	0.0250	0.0190	0.0110	0.0080	0.0112	fractional decomposition per month
maximum root-system nitrogen uptake rate	685.00	495.00	625.00	625.00	47.00	$\text{gN m}^{-2} \text{ month}^{-1}$
immobilization rate coefficient	12.90	10.00	20.50	53.00	9.75	maximum gN immobilized per gC of r_h

Table A2a: Biome-dependent parameters used in TEM-Hydro

parameter	description	temp. dec.	temp. conif.	boreal forest	shrub- land	grass- land	units
kc	CO ₂ response half-saturation constant	200	200	200	120	40	ppmv CO ₂
tmin	minimum temperature	0	-1	5	1	0	°C
toptmin	minimum topt	23	22	17	15.1	13	°C
toptmax	maximum topt	30.9	30	25	35.1	32.7	°C
tmax	maximum temp.	40	38	32	44	38	°C
sla ¹	specific leaf area	0.0242	0.00863	0.0137	0.0192	0.0356	m ² gC ⁻¹
href	reference height	6	6	6	3	6	meters
k _{rup}	half-saturation constant for vegetation n uptake (wrt root extent)	128.3	97.4	21.8	60.5	2.48	g rootC m ⁻²
k _{allom}	allometric coefficient for height	0.467	0.467	0.467	0.5	0.5	N/A
cn _{leaf}	C:N leaf	23.8	47.5	50	25	30.5	gC gN ⁻¹
cn _{sapwood}	C:N sapwood	300	500	500	200	34.5	gC gN ⁻¹
cn _{heartwood}	C:N heartwood	300	500	500	200	34.5	gC gN ⁻¹
cn _{root}	C:N root	44.6	57.7	50	49.7	40.5	gC gN ⁻¹
cn _{seed}	C:N seed	44.6	57.7	50	25	40.5	gC gN ⁻¹
fs _{aplive}	fraction of sapwood that is alive	0.17	0.07	0.07	0.13	0.5	gC living gC sapwood ⁻¹
phen	phenological class	1	0	0	0	2	0 = evergreen; 1 = cold- deciduous; 2 = stress- deciduous
w _{leaf}	width of leaf ²	0.01	0.002	0.002	0.01	0.005	meters
³ gsa	slope of photosynthesis-conductance relation	9	6	6	6	4	N/A
gs _{min}	min. stomatal conductance	10	10	10	10	25	mmol m ⁻² s ⁻¹
k _{ext}	extinction coefficient	0.5	0.5	0.5	0.3	0.5	fraction

albedo	albedo	0.18	0.14	0.14	0.21	0.2	fraction
lscmin	min. leaf specific conductance	0.1	0.1	0.1	0.25	0.25	$\text{mmol m}^{-2} \text{s}^{-1} \text{MPa}^{-1}$
groot	root hydraulic conductance	0.02	0.0269	0.0269	0.025	0.002	$\text{mmol gC}^{-1} \text{s}^{-1} \text{MPa}^{-1}$
kstem	sapwood hydraulic conductivity	200000	72200	72200	50000	50000	$\text{mmol m}^{-1} \text{s}^{-1} \text{MPa}^{-1}$
rhostem	C density in sapwood	250	209	209	250	250	gC m^{-3}
rootzc	constant coefficient for rooting depth	2	2	2	5	1.5	meters
vegtauleaf	leaf lifetime	1	2	2	2	1	years
vegtauroot	root lifetime	1	1	1	1	1	years
vegtauseed	seed lifetime	1	1	1	1	1	years
microbelcc lnc	reference C:N of litter, used to adjust decomposition rate	70.87	67.4	67.4	70.87	57.1	gC gN^{-1}
microbecn soil	target c:n of soil organic matter	20	20	29.73	11.9	11.12	gC gN^{-1}
vegcnltr	c:n of leaf litter	57.3	48.8	60	30	75	gC gN^{-1}
o3para	damage coefficient for ozone exposure	2.6	0.7	0.7	2.6	3.9	

¹Schulze, E. D., Kelliher, F. M., Korner, C., Lloyd, J., and Leuning, R. 1994. Relationships among maximum

²Choudhury, B. J. and Monteith, J. L. 1988. A four-layer model for the heat budget of homogenous land

³calibrated to match annual et (yreet)

Table A2b: Biome-independent parameters used in TEM-Hydro

parameter	description	value	units
ki	light response half-saturation constant	75	cal cm ⁻² day ⁻¹
¹ raalpha	respiration parameter regarding curve shape	0.01	N/A
¹ rabeta	minimum temperature of ra	-5	°C
¹ ragamma	maximum temperature of ra	55	°C
¹ raqref	reference "Q10" of ra	2.07	N/A
¹ ratref	reference temperature for ra	25	°C
kn1	half-saturation constant for vegetation n uptake (wrt N-concentration)	0.004 2	vsm ³ g AVLN (kg soil H2O) ⁻¹
² cdleaf	drag coefficient of leaf	0.1	N/A
³ rhalpha	respiration parameter regarding curve shape	0.009	N/A
³ rhbeta	minimum temperature of rh	-10	°C
³ rhgamma	maximum temperature of rh	100	°C
³ rhqref	reference "Q10" of rh	1.83	N/A
³ rhtref	reference temperature for rh	25	°C
kn2	half-saturation constant for microbial n uptake (wrt N-concentration)	0.004 2	
rssmin		400	
rssslope	increase in soil surface resistance with 1 mm of depletion below field capacity	40	s m ⁻¹ mm ⁻¹

¹Hanson, P. J., Amthor, J. S., Wullschleger, S. D., Wilson, K. B. Grant, R. F., Hartley, A., Hui, D., Hunt, E. R. Jr., Johson, J. S., King, A. W., Luo, Y., McNulty, S. G., Sun, G., Thornton, P. E., Wang, S., Williams, M., Baldocchi, D. D., and Cushman, R. M. 2004. Oak forest carbon and water simulations: model intercomparisons and evaluations against independent data. Ecological Monographs. 74(3): 443-489. (LaRs reference)

²Choudhury, B. J. and Monteith, J. L. 1988. A four-layer model for the heat budget of homogenous land surfaces. Quarterly Journal of the Royal Meteorological Society. 114: 373-398.

³Lloyd, J. and Taylor, J. A. 1994. On the temperature dependence of soil respiration. Functional Ecology. 8: 315-323.

Table A3: TEM-Hydro Target Values parameterization

Harvard Forest Coniferous (Temperate Coniferous Forest)

<i>Variable</i>	<i>Value</i>	<i>Units</i>	<i>Source</i>
VEGC	10800	gC m ⁻²	based on <i>McClougherty et al.</i> [1982; <i>Pastor et al.</i> [1984], and K.J. Nadelhoffer (unpublished data, 1991)
SOILC	8290	gC m ⁻²	based on <i>Gaudinski et al.</i> [2000] – all carbon above bottom of BW1 horizon
SOILN	414.5	gN m ⁻²	assume soil C:N ratio of 20
AVALN	1.9	gN m ⁻²	based on <i>Vitousek et al.</i> [1982]
NPP	600	gC m ⁻² yr ⁻¹	based on <i>McClougherty et al.</i> [1982; <i>Pastor et al.</i> [1984], and K.J. Nadelhoffer (unpublished data, 1991)
GPP	1130	gC m ⁻² yr ⁻¹	based on <i>Waring et al.</i> [1998]
NPPSAT	750	gC m ⁻² yr ⁻¹	assume N saturation effect is 25%
NUPTAKE	8.9	gN m ⁻² yr ⁻¹	based on Figure 2 of <i>Aber et al.</i> [1983] – assume N up = N min.
pleafc	0.42		same as for NPP
pstemc	0.25		same as for NPP
prootc	0.33		same as for NPP
LAI(target)	4.4		[<i>Barford et al.</i> , 2001]
yrEET	569	mm	Ltinternet website: http://intranet.ltinternet.edu/archives/documents/Publications/climdes/siteclim.toc.html

Harvard Forest Deciduous (Temperate Deciduous Forest)

<i>Variable</i>	<i>Value</i>	<i>Units</i>	<i>Source</i>
VEGC	17440	$\frac{\text{gC}}{\text{m}^2}$	based on <i>McClagherty et al.</i> [1982]; <i>Pastor et al.</i> [1984], and K.J. Nadelhoffer (unpublished data, 1991)
SOILC	8290	$\frac{\text{gC}}{\text{m}^2}$	based on <i>Gaudinski et al.</i> [2000] – all carbon above bottom of BW1 horizon
SOILN	414.5	$\frac{\text{gN}}{\text{m}^2}$	assume soil C:N ratio of 20
AVALN	2.2	$\frac{\text{gN}}{\text{m}^2}$	based on <i>Vitousek et al.</i> [1982]
NPP	730	$\frac{\text{gC}}{\text{m}^2 \text{ yr}^{-1}}$	based on <i>McClagherty et al.</i> [1982]; <i>Pastor et al.</i> [1984], and K.J. Nadelhoffer (unpublished data, 1991)
GPP	1380	$\frac{\text{gC}}{\text{m}^2 \text{ yr}^{-1}}$	based on <i>Waring et al.</i> [1998]
NPPSA T	912.5	$\frac{\text{gC}}{\text{m}^2 \text{ yr}^{-1}}$	assume N saturation effect is 25%
NUPTA KE	10.3	$\frac{\text{gN}}{\text{m}^2 \text{ yr}^{-1}}$	based on Figure 2 of <i>Aber et al.</i> [1983] – assume N up = N min.
pleafc	0.29		same as for NPP
pstemc	0.36		same as for NPP
prootc	0.35		same as for NPP
LAI(target)	4.4		[<i>Barford et al.</i> , 2001]
yrEET	569	mm	Lternet website: http://intranet.lternet.edu/archives/documents/Publications/climdes/siteclim.toc.html

Bonanza Creek (Boreal Forest)

<i>Variable</i>	<i>Value</i>	<i>Units</i>	<i>Source</i>
VEGC	9000	$\frac{\text{gC}}{\text{m}^2}$	[<i>Oechel and Van Cleve, 1986; Van Cleve et al., 1983</i>]
SOILC	11000	$\frac{\text{gC}}{\text{m}^2}$	[<i>Van Cleve et al., 1983</i>]
SOILN	370	$\frac{\text{gN}}{\text{m}^2}$	[<i>Van Cleve et al., 1983</i>]
AVALN	0.5	$\frac{\text{gN}}{\text{m}^2}$	
NPP	220	$\frac{\text{gC}}{\text{m}^2 \text{ yr}^{-1}}$	[<i>Van Cleve et al., 1983; Weber and Van Cleve, 1984</i>]
GPP	550	$\frac{\text{gC}}{\text{m}^2 \text{ yr}^{-1}}$	[<i>Viereck et al., 1983</i>]
NPPSA T	330	$\frac{\text{gC}}{\text{m}^2 \text{ yr}^{-1}}$	[<i>Chapin III et al., 1986; Van Cleve and Zasada, 1976</i>]
NUPTA KE	2.3	$\frac{\text{gN}}{\text{m}^2 \text{ yr}^{-1}}$	[<i>Oechel and Van Cleve, 1986; Van Cleve et al., 1983</i>]
pleafc	0.65		same as for NPP
pstemc	0.08		same as for NPP
prootc	0.27		same as for NPP
LAI(target)	2.65		[<i>Scurlock et al., 2001</i>]
yrEET	194	mm	Lternet website: http://intranet.lternet.edu/archives/documents/Publications/climdes/siteclim.toc.html

Pawnee Shortgrass Steppe (Shortgrass prairie)

<i>Variable</i>	<i>Value</i>	<i>Units</i>	<i>Source</i>
VEGC		gC m ⁻²	allow TEM to calculate – do not calibrate
SOILC	3436	gC m ⁻²	grandfathered
SOILN	309	gN m ⁻²	grandfathered
AVALN	2.0	gN m ⁻²	grandfathered
NPP	184	gC m ⁻² yr ⁻¹	[<i>Michunas and Laurenroth, 1992</i>]
GPP	357	gC m ⁻² yr ⁻¹	based on old GPP/NPP ratio of 1.94
NPPSAT	368	gC m ⁻² yr ⁻¹	assume N saturation effect is 100%
NUPTAKE	4.2	gN m ⁻² yr ⁻¹	[<i>Schimel et al., 1985</i>] average N mineralization for summit, backslope, and footslope
pleafc	0.21		same as for NPP
pstemc	0.23		same as for NPP
prootc	0.56		same as for NPP
LAI(target)	0.55		[<i>Knight, 1973</i>]
yrEET	372	mm	

Curlew (Xeric Shrubland)

<i>Variable</i>	<i>Value</i>	<i>Units</i>	<i>Source</i>
VEGC	540	gC m ⁻²	[Caldwell et al., 1977]
SOILC	2500	gC m ⁻²	[Bjerregaard, 1971; McGuire et al., 1995]
SOILN	210.1	gN m ⁻²	[Bjerregaard, 1971]
AVALN	1.6	gN m ⁻²	[Gist et al., 1978]
NPP	110	gC m ⁻² yr ⁻¹	[Caldwell et al., 1977; Raich and Nadelhoffer, 1989]
GPP	235	gC m ⁻² yr ⁻¹	[Caldwell et al., 1977]
NPPSAT	120	gC m ⁻² yr ⁻¹	[Lajtha and Whitford, 1989]
NUPTAKE	2.7	gN m ⁻² yr ⁻¹	[McGuire et al., 1995]
pleafc	0.2		same as for NPP; also based on [Knapp, 1985]
pstemc	0.19		same as for NPP; also based on [Knapp, 1985]
prootc	0.6		same as for NPP
LAI(target)	2.08		[Scurlock et al., 2001]
yrEET	152	mm	

References

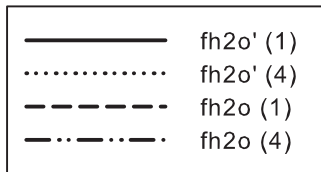
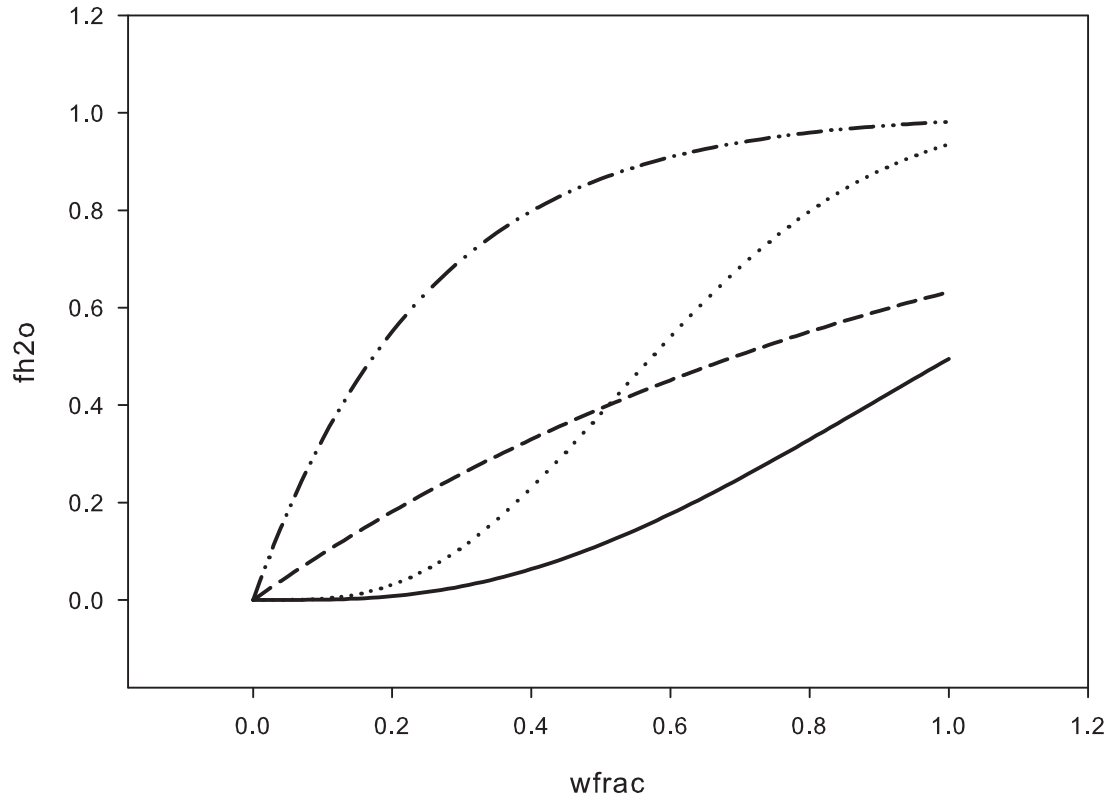
- Aber, J. D., et al. (1983), Potential sinks for mineralized nitrogen following disturbance in forest ecosystems, *Ecological Bulletin (Stockholm)*, 35, 179-192.
- Barford, C. C., et al. (2001), Ecological measurements to compliment eddy-flux measurements at Harvard Forest.
- Bjerregaard, R. S. (1971), The Nitrogen Budget of Two Salt Desert Shrub Communities of Western Utah, Utah State University, Logan.
- Caldwell, M. M., et al. (1977), Carbon balance, productivity, and water use of cold-winter desert shrub communities dominated by C3 and C4 species, *Oecologia*, 29, 275-300.
- Chapin III, F. S., et al. (1986), The nature of nutrient limitation in plant communities, *The American Naturalist*, 127(1), 48-58.
- Gaudinski, J. B., et al. (2000), Soil carbon cycling in a temperate forest: radiocarbon-based estimates of residence times, sequestration rates and partitioning of fluxes, *Biogeochemistry*, 51, 33-69.
- Gist, C. S., et al. (1978), A computer simulation model of nitrogen dynamics in a Great Basin desert ecosystem, in *Nitrogen in Desert Ecosystems*, edited by N. E. West and J. Skujins, pp. 182-206, Dowden, Hutchinson and Ross, Stroudsburg, PA.
- Knapp, A. K. (1985), Effect of fire and drought on the ecophysiology of *Andropogon gerardii* and *Panicum vergatum* in a tallgrass prairie, *Ecology*, 66(4), 1309-1320.
- Knight, D. H. (1973), Leaf area dynamics of a shortgrass prairie in Colorado, *Ecology*, 54(4), 891-896.
- Lajtha, K., and W. G. Whitford (1989), The effect of water and nitrogen amendments on photosynthesis, leaf demography, and resource-use efficiency in *Larrea tridentata*, a desert evergreen shrub, *Oecologia*, 80, 341-348.
- McClougherty, C. A., et al. (1982), The role of fine roots in the organic matter and nitrogen budgets of two forested ecosystems, *Ecology*, 63, 1481-1490.
- McGuire, A. D., et al. (1995), Equilibrium responses of soil carbon to climate change: empirical and process-based estimates, *Journal of Biogeography*, 22, 785-796.
- Michunas, D. G., and W. K. Laurenroth (1992), Carbon dynamics and estimate of primary production by harvest, ^{14}C dilution, and ^{14}C turnover, *Ecology*, 73(2), 593-607.
- Oechel, W. C., and K. Van Cleve (1986), The role of bryophytes in nutrient cycling in the taiga, in *Forest Ecosystems in the Alaskan Taiga*, edited by K. Van Cleve, et al., pp. 121-137, Springer-Verlag, New York.
- Pastor, J., et al. (1984), Biomass prediction using generalized allometric regressions for some Northeast tree species, *Forest Ecol. Manag.*, 7(265-274).
- Raich, J. W., and K. J. Nadelhoffer (1989), Belowground carbon allocation in forest ecosystems: Global trends, *Ecology*, 70, 1346-1354.
- Schimel, D. S., et al. (1985), Biogeochemistry of C, N, and P in as soil catena of the shortgrass steppe, *Ecology*, 66(1), 276-283.
- Scurlock, J. M. O., et al. (2001), Global Leaf Area Index Data from Field Measurements, 1932-2000., Oak Ridge National Laboratory, Oak Ridge, TN.
- Van Cleve, K., and J. Zasada (1976), Response of 70-year-old white spruce to thinning and fertilization in interior Alaska, *Can. J. For. Res.*, 6, 145-152.

- Van Cleve, K., et al. (1983), Productivity and nutrient cycling in taiga forest ecosystems, *Can. J. For. Res.*, *13*, 747-766.
- Viereck, L. A., et al. (1983), Vegetation, soils, and forest productivity in selected forest types in interior Alaska, *Can. J. For. Res.*, *13*, 703-720.
- Vitousek, P. M., et al. (1982), A comparative analysis of potential nitrification and nitrate mobility in forest ecosystems, *Ecological Monographs*, *52*, 155-177.
- Waring, R. H., et al. (1998), Net primary production of forests: a constant fraction of gross primary production?, *Tree Physiol.*, *18*, 129-134.
- Weber, M. G., and K. Van Cleve (1984), Nitrogen transformations in feather moss and forest floor layers of interior Alaska black spruce ecosystems, *Can. J. For. Res.*, *14*, 278-290.

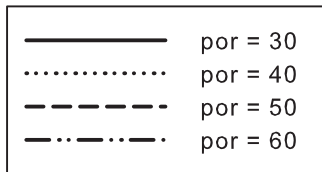
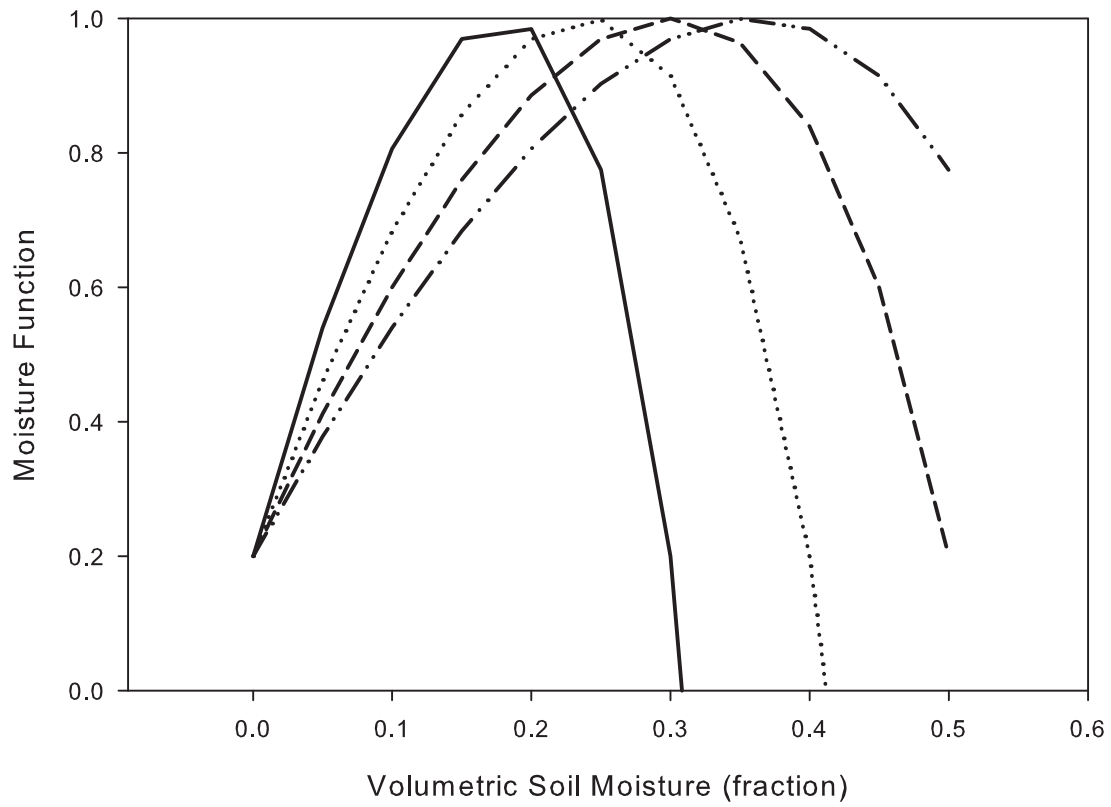
Table A4: River basins used for model checking

Station Name	Area (km²)	Biome	
Pantano Wash near Vail, AZ	1169.92	Grass	
Paria R. at Lees Ferry, AZ	3609.60	Shrub	
Salt R. near Roosevelt, AZ	11023.36	Shrub	
Maggie Ck above Maggie Ck Canyon near Carlin,NV	849.92	Grass	
South Fork Humboldt above Tenmile Ck near Elko, NV	2298.88	Shrub	
Rock Ck near Battle Mountain, NV	2211.20	Grass	
Bruneau R. at Rowland, NV	977.92	Grass	
Little Colorado near Cameron, AZ	67735.04	Shrub	
Verde R. below Tangle Creek, above Horseshore Dam, AZ	14996.48	Shrub	
Big Sandy R. near Wikieup, AZ	7019.52	Shrub	
Little Colorado R. at Woodruff, AZ	20664.32	Shrub	
Muddy R. near Moapa, NV	9779.20	Shrub	
AMERICAN R A FAIR OAKS CA	4717.54	Trees	
EEL R A FORT SEWARD CA	5319.34	Trees	
TRINITY R NR BURNT RANCH CA	3737.49	Trees	
UNCOMPAHGRE RIVER AT DELTA, CO.	2718.01	Trees	
GUNNISON RIVER NEAR GUNNISON, CO.	2133.51	Trees	
WHITE RIVER BELOW MEEKER, CO	2747.72	Trees	
NF CLEARWATER RIVER NR CANYON RANGER STATION ID	3730.83	Trees	
SF CLEARWATER RIVER AT STITES ID	3101.54	Trees	
Bitterroot River near Darby MT	2843.77	Trees	
TRUCKEE R AT RENO,NV	2776.47	Trees	
MIDDLE FORK WILLAMETTE RIVER AT JASPER, OR	3750.44	Trees	
ROGUE RIVER AT DODGE BRIDGE, NEAR EAGLE POINT, OR	2905.89	Trees	
SANTIAM RIVER AT JEFFERSON, OR	4402.15	Trees	
COLVILLE RIVER AT KETTLE FALLS, WA	2547.29	Trees	
COWLITZ RIVER BELOW MAYFIELD DAM, WA	3572.83	Trees	
SNOHOMISH RIVER NEAR MONROE, WA	3992.59	Trees	

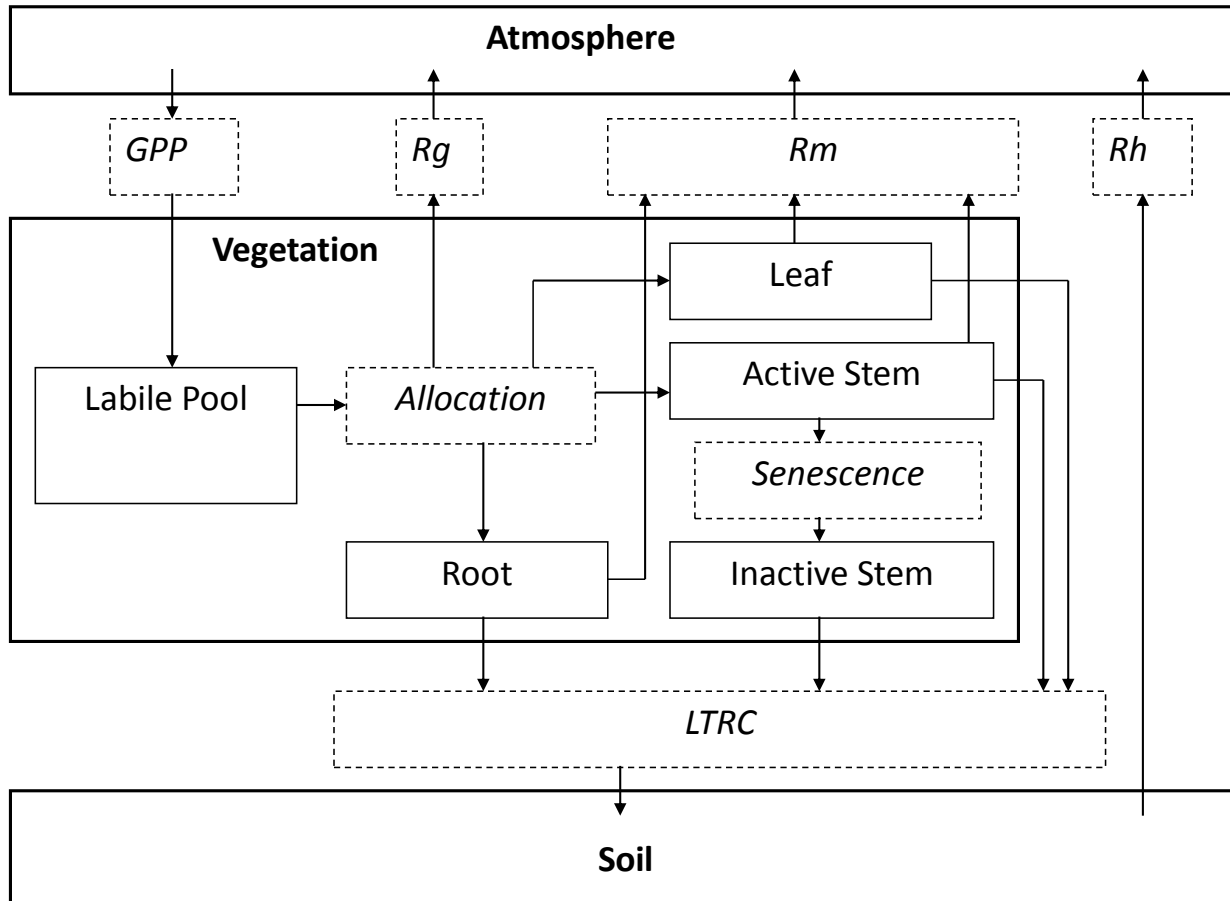
Moisture Stress Function



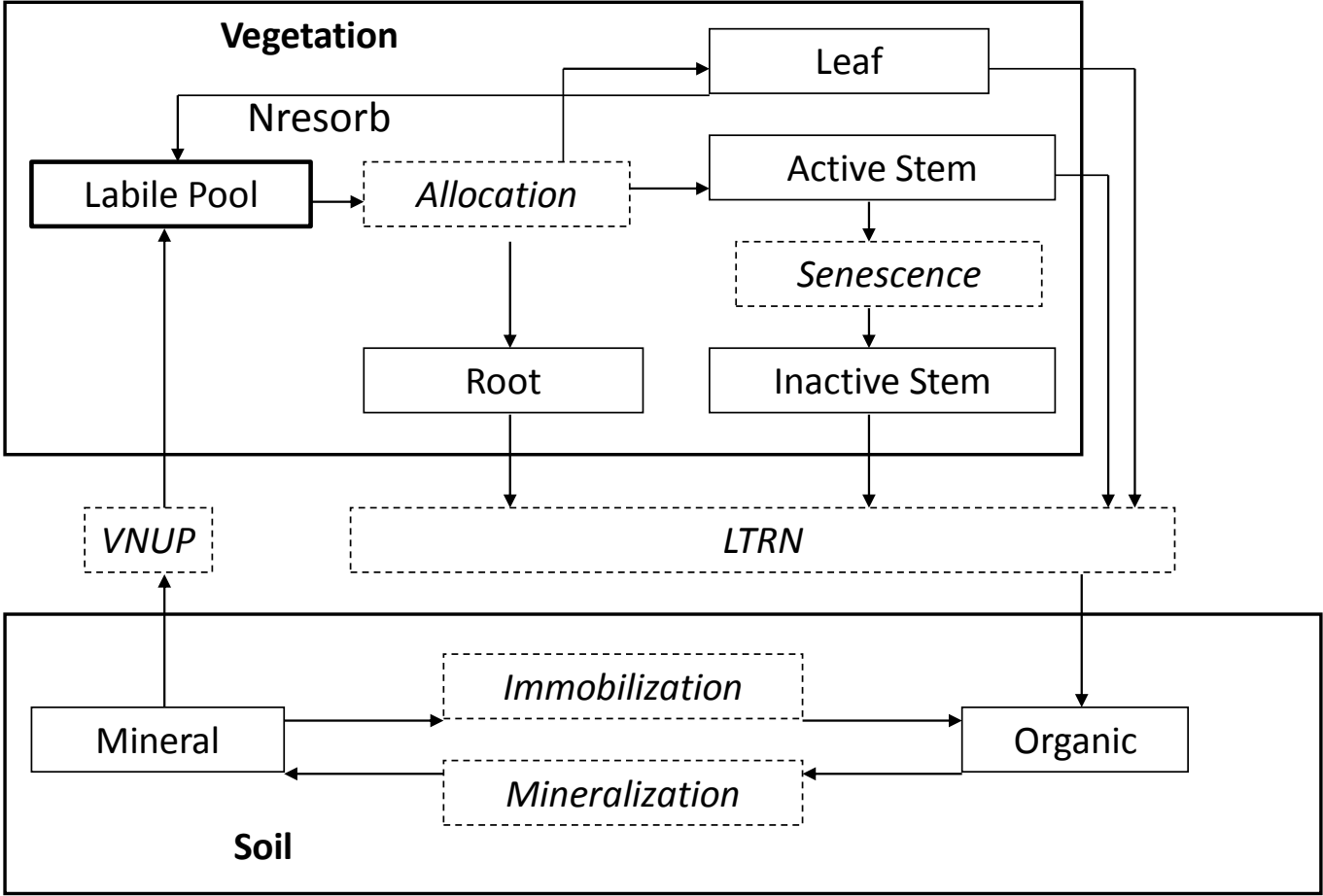
Moisture Function for R_h



Carbon



Nitrogen



Water

Shuttleworth-Wallace method

- Screen height, known T, VPR
- Canopy airspace, in contact with leaves and soil
- Surface of "big leaf"
- Soil Surface

